Examining Environmental Changes on Concrete Bridges with the Help of Local Distance Correlation

CARINA BEERING

ABSTRACT

To investigate the influence of environmental effects on concrete bridges, local distance correlation (LDC) is used due to its ability to accommodate the nature of environmental data, namely local stationarity. Similarities and differences of these influential variables can be identified with the help of LDC. Moreover, LDC pattern based upon weather phenomena and natural frequencies as well as crack widths show relations between their respective temporal progresses. These findings are illustrated by data from a test bridge in Munich and a bridge for vehicles in Bochum, Germany.

INTRODUCTION

The environment changes constantly, be it the temperature or other weather conditions as rain or wind. Thus, civil structures like bridges are subjected to these changes without cease. In a time where climate change is one of the biggest challenges, it is highly important to understand the consequences environmental alterations have on these buildings. Moreover, finding patterns in the bridge's reaction to changes in weather condition help to distinguish reversible adjustments from actual defects. In addition to that, predictions of future reactions to more extreme weather conditions could help to ensure the safety of our infrastructural buildings. Statistical methods offer various tools to analyze sensor data in order to find these patterns. But not all of those are equally suitable. A classical approach is to observe the correlation between signals emitted from both the structure and weather stations. However, with this procedure, we are only able to captures linear dependencies. In consequence, the correlation is blind for more complex dependence structures like quadratic dependencies. Here, the concept of distance correlation as introduced by [1] comes into play. It is not only not restricted to linear dependence, but is also able to detect independence and does not require normality. Additionally, most sensor data is non-stationary. In view of temperature, we observe seasonal effects and daily patterns, which lead to changes in mean and variance over time. Yet, looking at small time frames, the behavior can be described as stationary. Hence,

Carina Beering, Email: beeringc@hsu-hh.de. Research group of Mathematics and Statistics, Helmut- Schmidt-Universität/Universität der Bundeswehr Hamburg, Germany

the data is considered as locally stationary. This is the reason why we use the extension of [2] of the original version of distance correlation, the so-called LDC, to investigate the impact changes in natural conditions have on concrete bridges. In particular, we use data from a test bridge of the University of the Bundeswehr Munich as well as data provided by the TU Dortmund University originating from a bridge for vehicles in Bochum.

The paper is structured as follows: First, a more detailed description of the LDC and its components as well as their empirical counterparts are provided. Subsequently, the real-world scenarios, where the statistical concepts of the previous section are applied, is presented. Lastly, conclusions close the paper.

LOCAL DISTANCE CORRELATION

The concept of distance correlation has evolved in several steps: Originally introduced by [1] to deal with independent and identically distributed data, [3] attuned the concept stationary data. This, again, paved the way for [2], who refined the former modification to be appropriate for local stationary time series, resulting in the LDC. The last version meets the requirements structural health data imposes. In consequence, we consider two locally stationary processes $(Y_{t,T})_{t=1}^{T}$ and $(Z_{t,T})_{t=1}^{T}$ for $T \in \mathbb{N}$ as proposed by [4], which suffice the assumptions of [2]. Hence, given a time point $u \in [0,1]$, we can approximate the original processes locally in a neighborhood of u by the respective strictly stationary companion processes $\left(\widetilde{Y}_t(u)\right)_{t\in\mathbb{Z}}$ and $\left(\widetilde{Z}_t(u)\right)_{t\in\mathbb{Z}}$. To slim down the notation, we focus on the one-dimensional case plus the contemporaneous contemplation of the two processes. For a more flexible approach in the time domain, see [5]. As the characteristic functions of the companion processes are fundamental for all versions of distance correlation, consider for $s_1, s_2 \in \mathbb{R}$

$$\varphi_Y(u; s_1) := Ee^{is_1\widetilde{Y}_0(u)} \quad \text{and} \quad \varphi_Z(u; s_2) := Ee^{is_2\widetilde{Z}_0(u)} \tag{1}$$

together with the joint characteristic function

$$\varphi_{Y,Z}(u; s_1, s_2) := Ee^{is_1\widetilde{Y}_0(u)+is_2\widetilde{Z}_0(u)}. \tag{2}$$

Additionally, a weight function w is needed for the LDC, which we take up directly from [2], to wit

$$w(s_1, s_2) = (\pi s_1 s_2)^{-2} \tag{3}$$

for $s_1, s_2 \in \mathbb{R}\setminus\{0\}$. Thus, the weight function is always positive. Finally, the non-lagged local distance covariance as in [2] reads as follows:

$$\mathcal{V}^2_{Y,Z}(u) = \int_{\mathbb{R}\times\mathbb{R}} \left|\varphi_{Y,Z}(u; s_1, s_2) - \varphi_Y(u; s_1)\varphi_Z(u; s_2)\right|^2 w(s_1, s_2)\, ds_1 ds_2. \tag{4}$$

With $\mathcal{V}^2_{Y,Z}(u)$, the LDC is defined as

$$\mathcal{R}^2_{Y,Z}(u) = \begin{cases} \frac{\mathcal{V}^2_{Y,Z}(u)}{\sqrt{\mathcal{V}^2_{Y,Y}(u)\mathcal{V}^2_{Z}(u)}}, & \mathcal{V}^2_{Y,Y}(u)\mathcal{V}^2_{Z,Z}(u) > 0, \\ 0, & \mathcal{V}^2_{Y,Y}(u)\mathcal{V}^2_{Z,Z}(u) = 0. \end{cases} \tag{5}$$

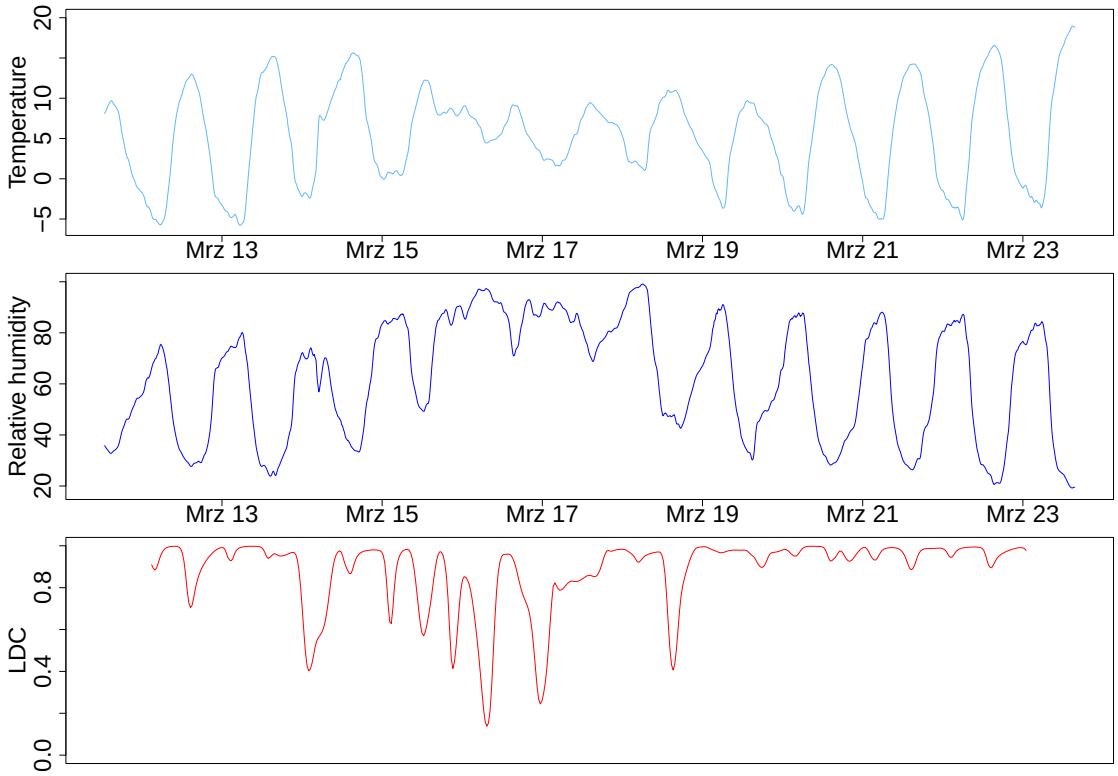

Figure 1. Temperature and relative humidity with their corresponding LDC.

Next, we need an empirical counterpart suitable for the use of data for (4) and (5) since the companion processes are not observable. To tie in with the afore-stated definitions, we borrow the ones of [2] de novo, starting with the introduction of the so-called local sample analogues of the characteristic functions in (4) and (5). Consequently, regard

$$\widehat{\varphi}_Y\left(u;s_1\right) := \frac{1}{b_T T}\sum_{t=1}^{T} K\left(\frac{{}^{t}\!/_{T}-u}{b_T}\right) e^{is_1 Y_{t,T}} \tag{6}$$

and

$$\widehat{\varphi}_Z\left(u;s_2\right) := \frac{1}{b_T T}\sum_{t=1}^{T} K\left(\frac{{}^{t}\!/_{T}-u}{b_T}\right) e^{is_2 Z_{t,T}} \tag{7}$$

plus the joint version

$$\widehat{\varphi}_{Y,Z}\left(u;s_1,s_2\right) := \frac{1}{b_T T}\sum_{t=1}^{T} K\left(\frac{{}^{t}\!/_{T}-u}{b_T}\right) e^{is_1 Y_{t,T}+is_2 Z_{t,T}}. \tag{8}$$

A kernel function K combined with a bandwidth b_T depending on the sample size T take care of the locality. Details concerning regularity conditions can be found in [2]. With the already defined weight function w from (3), the empirical local distance covariance states as

$$\widehat{\mathcal{V}}^2_{Y,Z}(u) = \int_{\mathbb{R}\times\mathbb{R}} \left|\kappa_T \widehat{\varphi}_{Y,Z}\left(u;s_1,s_2\right) - \widehat{\varphi}_Y\left(u;s_1\right)\widehat{\varphi}_Z\left(u;s_2\right)\right|^2 w\left(s_1,s_2\right)\, ds_1\, ds_2. \tag{9}$$

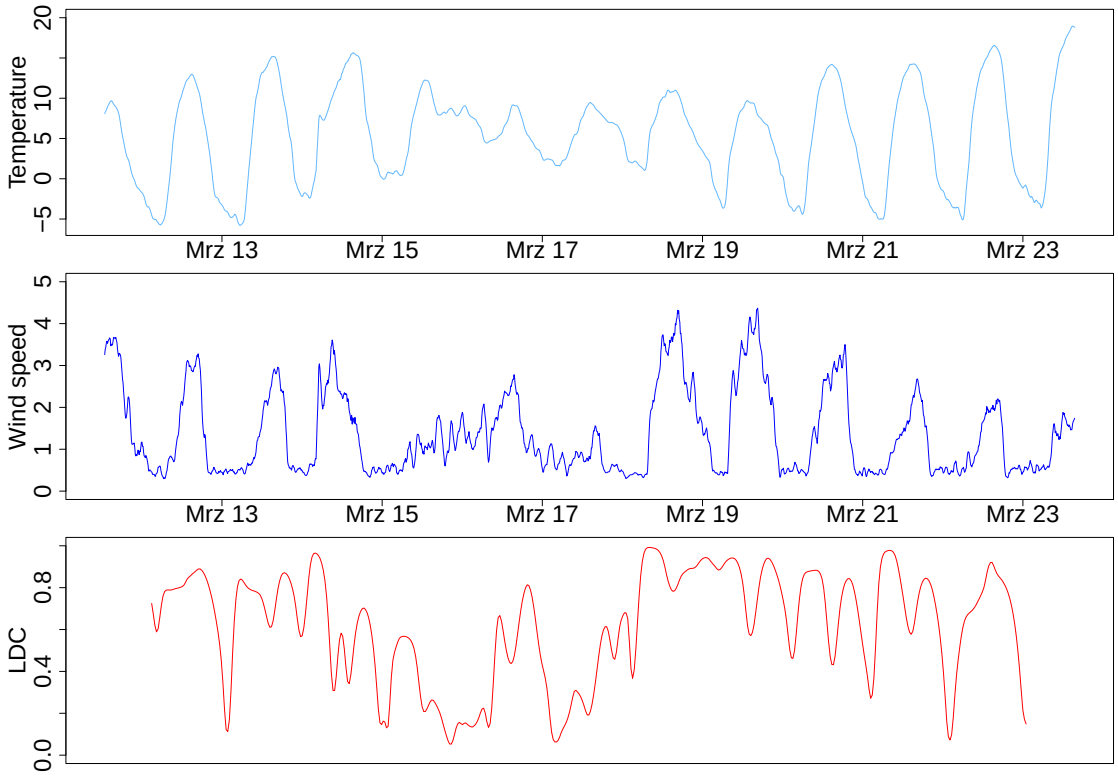

Figure 2. Temperature and wind speed with their corresponding LDC.

The additional factor κ_T compared to (4) is built as follows:

$$\kappa_T := \frac{1}{b_T T} \sum_{t=1}^{T} K\left(\frac{t/T - u}{b_T}\right). \tag{10}$$

An explication for the necessity of κ_T is provided in [2]. The empirical LDC is then obtained by

$$\widehat{\mathcal{R}}^2_{Y,Z}(u) = \begin{cases} \frac{\widehat{\mathcal{V}}^2_{Y,Z}(u)}{\sqrt{\widehat{\mathcal{V}}^2_{Y,Y}(u)\widehat{\mathcal{V}}^2_{Z,Z}(u)}}, & \widehat{\mathcal{V}}^2_{Y,Y}(u)\widehat{\mathcal{V}}^2_{Z,Z}(u) > 0, \\ 0, & \widehat{\mathcal{V}}^2_{Y,Y}(u)\widehat{\mathcal{V}}^2_{Z,Z}(u) = 0. \end{cases} \tag{11}$$

Consistency of these estimators is assured by Theorem 4.2 in [2], justifying their use in our study.

REAL-WORLD APPLICATIONS

Our first real-world application uses data from a 1997-built test bridge located at the University of the Bundeswehr Munich in Germany. The steel-concrete composite structure spans over a length of 30 meters and consists of two primary steel girders and nine transverse braces. For a more detailed description of both the bridge and the data-generating process, it is referred to [6].

We begin with the examination of the temporal course of different weather phenomena and their LDC by pairs over a time span of roughly two weeks in March 2022.

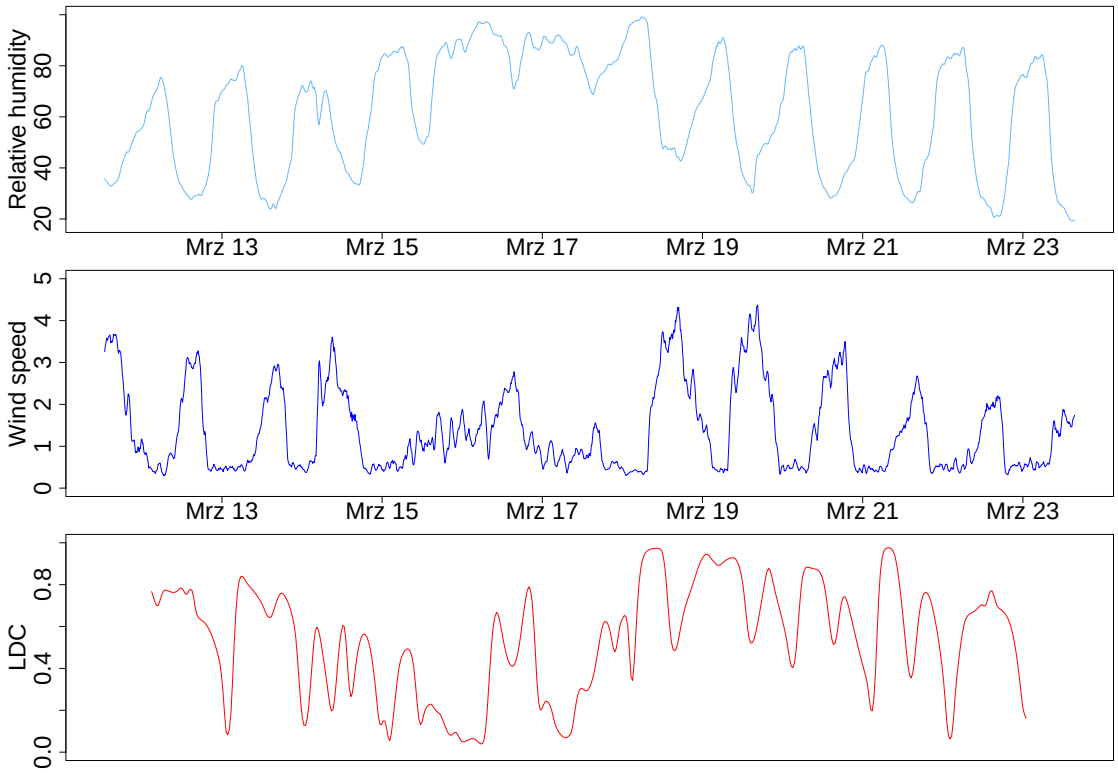

Figure 3. Relative humidity and wind speed with their corresponding LDC.

The idea is to determine whether the effects of a certain environmental factor can be explained by another to reduce the number of parameters taken into account for further analyses. For the computation of the local sample analogues of the different characteristic functions, an Epanechnikov kernel was used. Figure 1 shows the progress of environmental temperature in the first row, followed by the one of relative humidity. The last row displays the appurtenant LDC. The temperature follows a sinusoidal curve, where the course of each day is clearly visible. The pattern is quite regular except for a more troubled period around March 17. There, the daily peaks and lows are closer together and less extreme than before and after. Moreover, the curve is less sinusoidal. The relative humidity, on the other hand, reaches its highest values during the days around March 17. Again, this periods is distinctively different from the rest. However, we see the same sinusoidal pattern in the calmer times. The LDC mirrors the described particularities. Overall, the LDC is quite high but drops during the unsteady period in both temperature and relative humidity occurring around March 17. Thus, in quiet times, fluctuation pattern in relative humidity can be detected by identifying these changes in temperature or vice versa, justified by the LDC's high values. Nevertheless, this is not the case during rougher periods in the curves.

Moving on to Figure 2, the makeup stays the same, but wind speed has taken the place of relative humidity. However, the wind speed's progress shows a completely different behavior, resulting also in a completely different LDC pattern. Firstly, the sinusoidal pattern, though present, is far more jagged. Again, we notice the trouble period around March 17, but this time, the trajectory of the wind speed reaches peaks

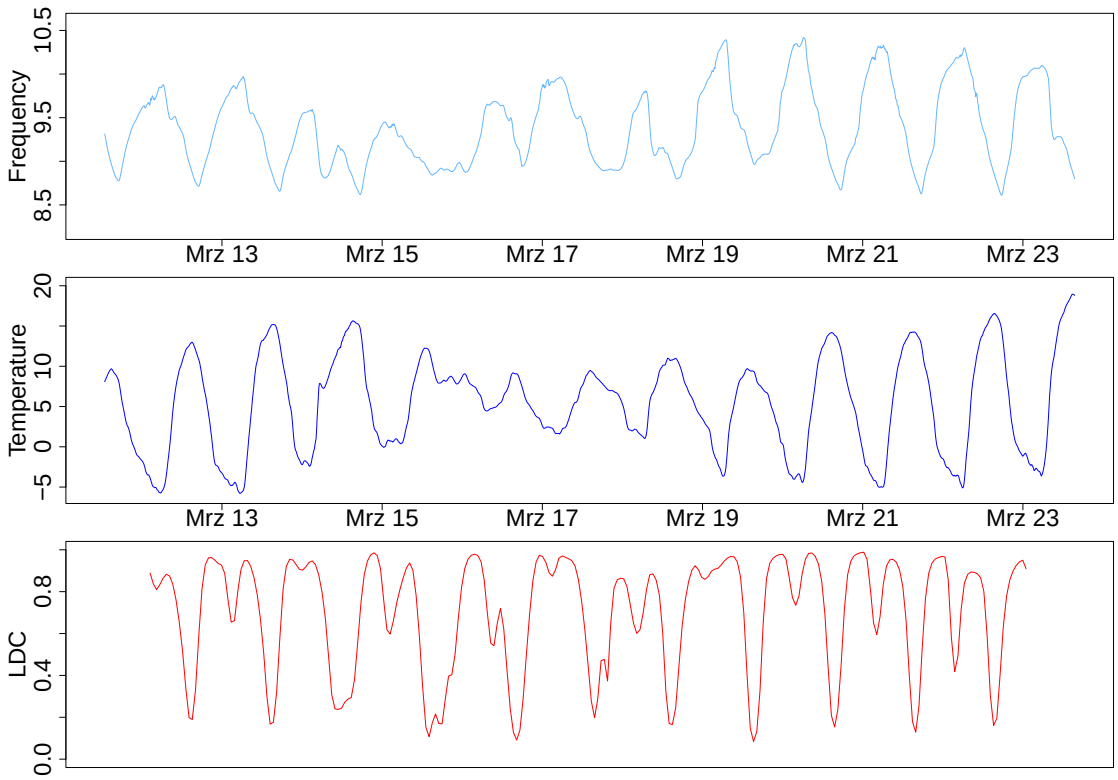

Figure 4. Natural frequency and temperature with their corresponding LDC.

well below compared to before and after. Due to the behavioral differences, the LDC follows a different pattern, too. Apart from the highs and lows around March 17, we also have a lot of changes on the other days. In consequence, it is not possible to deduce changes in wind speed from changes in temperature, as expected.

Lastly, Figure 3 sets relative humidity in relation to wind speed. The problematic phase of the 17th is standing out even less with this pairing. More generally, we have high variability in the LDC without being able to detect a distinct pattern, leading to the same conclusions as in the case above.

In sum, concerning these three environmental factors, we cannot exclude a certain factor from analyzing environmental effects on civil structures. However, regarding the temperature of the structure paired with the air temperature, a counterexample is presented in [5].

Next, we consider a pair consisting of temperature and natural frequency in order to find some similarities in their behavior. Figure 4 shows the progress of a natural frequency of the test bridge in the first row, whereas the temperature is displayed in the second. Again, we see a sinusoidal curve with pattern interruptions around March 17. Nevertheless, the LDC in the third row depicts a more regular pattern with less obvious interruptions in the trouble period. However, the values of the LDC show a wide range from high to low. By closer look, we see that the negative peaks of the frequency coincide with the temperature's positive peaks. Consequently, the LDC drops at exactly these turning points, where positive gradients at the one side fall together with negative ones on the other. For a more sound analysis, the air temperature could be replaced in

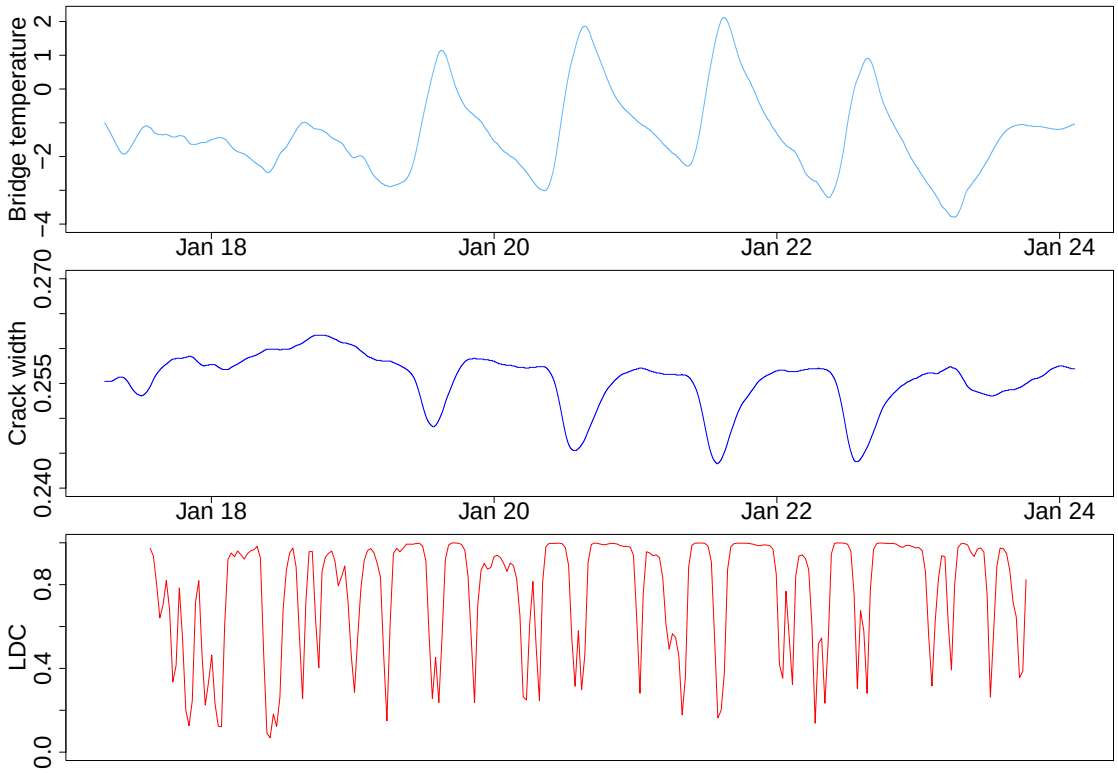

Figure 5. Bridge temperature and crack width with their corresponding LDC.

this scenario by the bridge temperature, if available. Another possibility would be to account for the time it takes for the concrete to adjust to temperature changes. This time can be determined via the method proposed in [5], involving LDC as well.

Moving on to the next real-world case, we use data from the project SFB 823, B5 of the German Research Foundation, which was generated on a concrete bridge for vehicles in Bochum, Germany, from 1961. The monitoring included crack widths at sixteen different locations plus environmental and bridge temperatures. For a detailed description of the monitoring process, see [7]. Figure 5 displays, from top to bottom, the bridge temperature curve, the progress of the width of a measured crack and their corresponding LDC during a week in January 2017. Comparing the LDC pattern with the two time series, we notice that moderate changes in temperature entails high LDC, while non-smooth changes in temperature involve a decrease of the LDC. Moreover, if there is a conversion of the temperature gradient, the LDC decreases as well, comparably to the frequency case. For a more extensive study regarding crack sizes, it is referred, once again, to [5].

CONCLUSIONS

The stochastic needs of environmental and structural health data are nicely met by local distance correlation. This efficient method highlights systematic similarities in time series beyond linearity or show their absence. It is applicable in various scenarios, making it prone to interdisciplinary cooperation, especially in the area of environmental

sciences and structural health monitoring.

ACKNOWLEDGMENT

This research is funded by dtec.bw - Digitalization and Technology Research Center of the Bundeswehr. dtec.bw is funded by the European Union - NextGenerationEU.

REFERENCES

1. Székely, G., M. Rizzo, and N. Bakirov. 2007. "Measuring and testing dependence by correlation of distances," *The Annals of Statistics*, 35:2769–2794.
2. Jentsch, C., A. Leucht, M. Meyer, and C. Beering. 2020. "Empirical characteristic functions-based estimation and distance correlation for locally stationary processes," *Journal of Time Series Analysis*, 41:110–133.
3. Davis, R., M. Matsui, T. Mikosch, and P. Wan. "Applications of distance correlation to time series," *Bernoulli*, 24.
4. Dahlhaus, R. 1997. "Fitting time series models to nonstationary processes," *The Annals of Statistics*, 25:1–37.
5. Beering, C. 2024. "Bridge Monitoring with the Help of Local Distance Correlation," *e-Journal of Nondestructive Testing*.
6. Jaelani, Y., A. Klemm, J. Wimmer, F. Seitz, M. Köhncke, F. Marsili, A. Mendler, M. von Danwitz, S. Henke, M. Gündel, T. Braml, M. Spannaus, A. Popp, and S. Keßler. 2021. "Developing a benchmark study for bridge monitoring," *Steel Construction*, 16(4):215–225.
7. Heinrich, J., R. Maurer, K. Leckey, C. Müller, and K. Ickstadt. 2021. "Detektieren ermüdungsbedingter Spannstahlbrüche mittels Rissmonitoring im Versuch und am Bauwerk," *Bauingenieur*, 90(3).